

Recognizing Slow Eye Movement for Driver Fatigue Detection with Machine Learning Approach

Yingying Jiao, Yong Peng and Bao-Liang Lu*
Department of Computer Science and Engineering
Key Laboratory of Shanghai Education Commission for
Intelligent Interaction and Cognitive Engineering
Shanghai Jiao Tong University, China

Xiaoping Chen*, Shanguang Chen, and Chunhui Wang
National Key Laboratory of Human Factors Engineering
China Astronaut Research and Training Center
Beijing, China

Abstract—Slow eye movement (SEM) regarded as a sign of onset of sleep is very significant for detecting driver fatigue, but its characteristics and detection algorithm have been rarely involved in the study of driver fatigue detection. In this study, some new features were extracted based on wavelet singularity analysis and statistics to detect SEMs. Six subjects participated in this simulated driving experiment, and for each subject, a more than 2 hours electro-oculogram (EOG) session was recorded. Each session was divided into SEM epochs and non-SEM epochs according to the common judgments made by the two of three experts by the visual recognition criteria of SEMs. Regarding the problem of detecting SEMs as an imbalance classification problem, and through the under-sampling and over-sampling methods a 2s horizontal electro-oculogram (HEO) signal could finally be recognized as the category of SEMs or non-SEM with the classifiers SVM, GELM, and KNN respectively. Results prove that the proposed features was a little better than the wavelet energy features, and through the combination of the wavelet energy features and the new features based on wavelet singularity analysis and statistics, the classification results were improved obviously.

I. INTRODUCTION

Slow eye movement (SEM) has been proved to be a reliable indicator of sleep onset, and was studied in a number of various kinds of sleep related researches [1, 2, 5, 7]. Because SEM appears during the wake-sleep transition, so it is very significant to study SEM in a real driving condition to avoid traffic accidents.

Blinks, saccades and fixation are the main ways of eye movements in wakefulness of human. The relationship between EOG and driver fatigue has been studied long time ago. However, little attention is being given to the characteristics of SEM about fatigue driving, and the specific description of SEM, such as what is the eye state (open or closed?) when it occurs, is insufficiency. Our experiments found that SEM could happen in the case of frequent continuous long blinks because of feeling sleepy and most happened during the period with eyes closed when people were in a state of severe drowsiness and could not control the trend of drooping eyelids.

For overlong eye lid closures (more than 3 seconds), there is no method to detect them. The conventional detection method for EOG is only according to the waveform in vertical electro-oculogram (VEO), but it can not distinguish it from an

upward glance followed by a downward glance [8, 9]. And in the condition of serious squint, the waveform caused by eyes closing and the following waveform caused by eyes opening in VEO are not obvious and very difficult to recognize. For the video detection method, it can not distinguish the driver's sleepy state from brief eye closure due to other reasons [10]. When the driver is awake and close his/her eyes, the SEMs will not appear, but when the driver is very sleepy and closes eyes at this movement, the SEM will appear in HEO [11, 12]. However, at this movement, the waveform of SEM in the HEO is very clear and easy to recognize. So detecting SEMs in HEO is very significant for judging the driver's current fatigue state.

To detect driver fatigue, algorithms for automatic recognizing SEMs have been rarely reported to our best knowledge. In sleep research field, there exist some methods, but these methods were are not satisfactory. In 1999, a linear regression method was used for the detection of SEM, and it was reported that the cycle length of SEM was shorter at stage wake than at sleep stages 1 and 2 [6]. In 2006, Elisa Magosso developed a wavelet based method, which was under the assumption that energy distribution was modified during SEM epochs according to the observation of experimental data [3]. SEMs could be detected through a discriminate function, which was defined as the ratio of specific energy combinations at lower frequencies with respect to both lower and higher frequency components. In [5], it simply judged SEMs or non-SEM by the amplitude threshold and the mean velocity threshold in a simulated driving task.

In essence, the previous work used the wavelet energy features and statistics features to detect SEMs, but seldom involved in the machine learning methods, in this study, new features based on wavelet singularity analysis and statistics such as entropy were proposed, and machine learning methods are introduced. For the classification, Support vector machines (SVMs) have been extensively used in widespread applications and were proved to have good generalization ability. The discriminative graph regularized Extreme Learning Machine (GELM) also is used to improve the performance based on the idea that similar samples should share similar properties and were proved to achieve much performance gain over standard ELM [13]. Therefore, by using these classifiers, our proposed features and the existing wavelet energy features are evaluated respectively. Experiments results found the performance of the new proposed features was slightly better than wavelet energy features. And through the combination of new features

* Corresponding authors: B. L. Lu (blu@sjtu.edu.cn); X. P. Chen (x-chen2009@163.com)

and wavelet energy features, the classification results can be improved obviously. This paper is organized as follows: In Section 2, the new features for recognizing SEMs are proposed, which are based on wavelet singularity analysis and statistics. And the overall processing procedure for classification using SVM, GELM and KNN is presented. Section 3 introduces the materials of the simulated driving experiments and gives a detail description of the characteristics of SEMs. Section 4 presents the experiments results and discussion. Section 5 concludes this work.

II. COMPUTER ANALYSIS PROCEDURE

The horizontal electro-oculogram (HEO) signal is calculated as the difference between the two convectional channels near the outer canthi of eyes. As can be seen in Fig. 1, one HEO signal session is divided into pieces of window data of length t (such as $t=2$ seconds) with a sliding step of length s , s and t could be set by user. For each window data, new features are defined and extracted based on wavelet transformation and other statistical parameters. By training classifiers, each window data will be classified as the category of SEMs or non-SEMs.

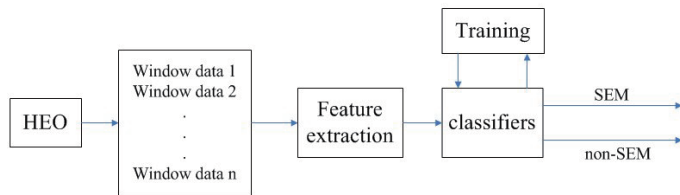


Fig. 1. The chart of computer analysis procedure

The labels of SEMs epochs and non-SEM epochs in HEO need to be marked manually. Eye movements were recognized as SEMs by visual experts if they meet the following criteria [3]: (1) slow sinusoidal excursion (0.2-0.6Hz) lasting more than one second; (2) amplitude between 20 and 200uV; (3) binocular synchrony with opposed-phase deflections in the two channels; (4) onsets of the right and left eye movement occur within 300ms of one another; (5) absence of artifacts; These criteria are commonly adopted for visual recognition of slow eye movements, which can be seen in Fig. 2 The rest HEO epochs which did not meet these criteria were labeled as non-SEMs. Then, the SEMs epochs and non-SEM epochs were divided into many 2s window data to form the original data samples.

A. New features

In this section, the features based on wavelet singularity analysis and some new statistics features are proposed.

1) *wavelet transformation*: The wavelet is a smooth and quickly vanishing oscillating function with good localization in both frequency and time [4]. A wavelet family $\psi_{a,b}(t)$ is the set of elementary functions generated by dilations and translations of a unique admissible mother wavelet $\psi(t)$:

$$\psi_{a,b}(t) = \frac{1}{\sqrt{|a|}} \psi\left(\frac{t-b}{a}\right) \quad (1)$$

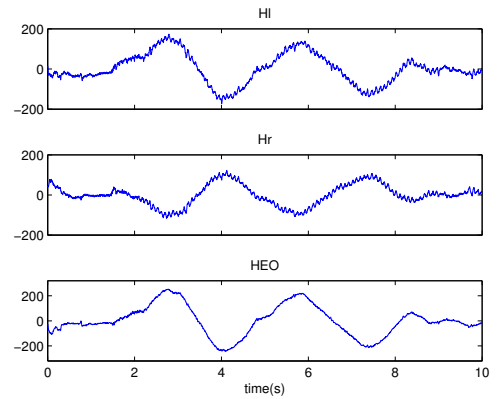


Fig. 2. A SEM example: Hl: the electrode near the outer canthus of left eye; Hr: the electrode near the outer canthus of right eye; HEO: The minus of Hl and Hr.

where $a, b \in \mathbb{R}$, $a \neq 0$, a, b are the scale and translation parameters, respectively, and t is the time. If the parameters (a, b) are continuous value, the transform is called continuous wavelet transform. Otherwise, if the parameters are discrete such as $a = a_0^j, b = kb_0 a_0^j$, that will be called the Discrete Wavelet Transform (DWT) basis as follows:

$$\psi_{j,k}(t) = a_0^{-j/2} \psi(a_0^{-j}t - kb_0), j, k \in F \quad (2)$$

If $\psi_{j,k}$ constitute the orthogonal wavelet basis of $L(\mathcal{R})$, for an arbitrary signal sample $f(t)$, the following equation exists:

$$f_w(t) = \sum_j \sum_k C_j(k) \psi_{j,k}(t) \quad (3)$$

where $C_j(k) = \langle f_w(t), \psi_{j,k}(t) \rangle$

2) *Features based on wavelet singularity analysis*: In digital signal processing, singularity detection of time series has important meaning, because these singularities contain the important information about the instantaneous change of signal [14, 15, 17]. Wavelet transform has a strong ability in detecting singularity and has been widely used. Because the eye movement is mostly a momentary behavior, and when saccades or blinks happen, the signal waveform will present some mutation points. However, the waveforms of SEMs are relatively smooth, without obvious mutation points. So, the continuous wavelet transform method for singularity analysis was chosen to identify SEMs in HEO.

$$\psi(t) = \left(\frac{2}{\sqrt{3}}\pi^{-1/4}\right) (1-t^2) e^{-t^2/2} \quad (4)$$

Mexican hat wavelet, as a commonly used wavelet base, its function (Eq. (4)) is proportional to the second derivative function of Gaussian probability density function, and has even symmetry structure, as can be seen in Fig. 3. If this function with even symmetry structure is used to do the convolution with an abrupt change point with local even symmetry, the convolution result will be local even symmetry. Otherwise, the result will be local odd symmetry.

Actually, continuous wavelet transform of the signal with Mexican hat mother wavelet is equal to making convolution

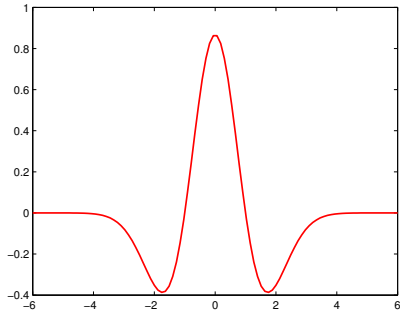


Fig. 3. Mexican Hat Wavelet.

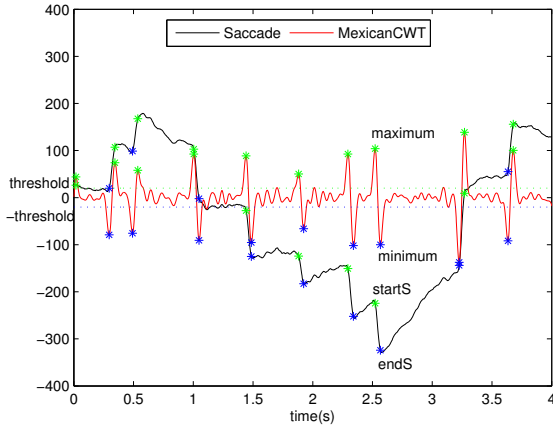


Fig. 4. Continuous wavelet transform of eye saccade activities based on Mexican hat mother wavelet.

between the signal and Mexican hat wavelet with the scaled and translated variables. For Mexican hat mother wavelet function (Eq. (4)), if a is its scaled variable, and b is its translated variable (like in Eq. (1)), as the change of the scale a , the corresponding maximum and minimum in continuous wavelet transform curve of original signal have a little difference. Along with the increase of the scale a , the local maximum and minimum points on the continuous wavelet transform curve become farther from the starting and ending points of saccade in HEO. So, according to the testing on training set, the scale a was set to 8 for continuous wavelet transformation.

In Fig. 4, the black curve is the original signal containing saccade activities and the red curve is the continuous wavelet transformation of the original signal. The green stars in the red curve represent the maximums and the blue stars represent the minimums, and in the black curve the corresponding green stars and blue stars represent the starting points of saccade activities or the ending points of saccade activities. In Fig. 4, for a saccade activity s_i , which begins at the point $startS$ and ends with the point $endS$, and in the red curve if the corresponding maximum point of $startS$ is above the threshold and the corresponding minimum point of $endS$ is below the minus threshold, this saccade activity s_i is selected to form the whole saccade activities $S=[s_1, s_2, \dots, s_n]$. The corresponding length sequence for the S is $L=[l_1, l_2, \dots, l_n]$.

We first calculated the difference of each saccade s_i in

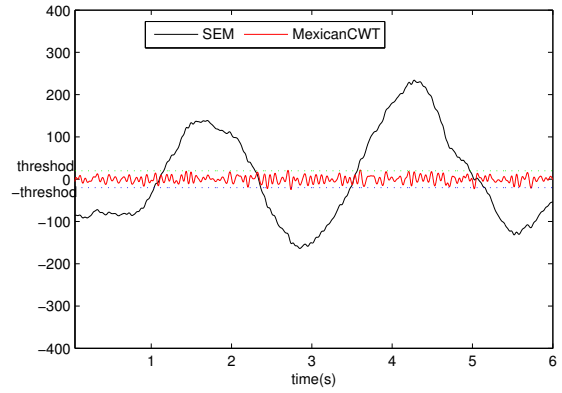


Fig. 5. Continuous wavelet transform of slow eye movements (SEMs) based on Mexican hat mother wavelet.

S , then calculated the absolute value of the maximum of this difference as m_i and the absolute value of the mean of this difference as e_i , so the corresponding vector $M=[m_1, m_2, \dots, m_n]$ and $E=[e_1, e_2, \dots, e_n]$ are formed; The maximum in M was defined as M_f , the mean of the E was defined as E_f and P_f was defined as $E * L^T$; And the variance V_f of the corresponding continuous wavelet transformation of this HEO is calculated. So, the features based on wavelet singularity analysis are:

$$F_1 = [M_f, E_f, P_f, V_f] \quad (5)$$

If there are no green stars and blue stars outside the range $[threshold, -threshold]$ like in Fig. 5, then the values of corresponding features in Eq. (5) were all set to zero .

3) *Features based on statistics*: For each window data of 2s HEO, the following statistical features were extracted: a) The mean A_1 , the variance A_2 and the entropy A_3 of the amplitude of signal. b) The mean D_1 , the variance D_2 and the entropy D_3 of the difference of signal. c) The absolute value of the difference between the maximum and the minimum of the amplitude of signal, denoted by M_3 . Entropy is a thermodynamic quantity describing the amount of disorder in the system. It is used as a measure of the degree of order/disorder of signal, so it can provide useful information about the underlying dynamical process associated with the signal. In Fig. 6, the histogram of the signal amplitude and the entropy is calculated according to the amplitude probability distribution. The more uniform the distribution of the amplitude, the greater its entropy value. So the features based on statistics is:

$$F_2 = [A_1, A_2, A_3, D_1, D_2, D_3, M_3] \quad (6)$$

The new features proposed in this study is defined as follows:

$$F_{DF} = [F_1, F_2] \quad (7)$$

4) *Features based on wavelet energy* : Magosso *et.al.* [3] used the wavelet energy to detect SEMs in sleep related research. These wavelet energy features also were used in our study to evaluate their performance. When frequency information is needed instead of the scales [14].

$$F_a = \frac{F_c}{\delta a} \quad (8)$$

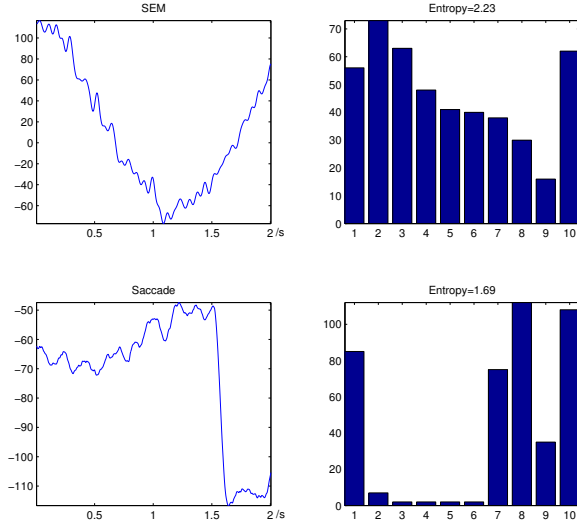


Fig. 6. The histogram of amplitude and the entropy

where F_a is the pseudo-frequency corresponding to scale a in Hz, a the scale, δ the sampling period, and F_c is the center frequency or dominant frequency of a wavelet in Hz, defined as the frequency with the highest amplitude in the Fourier transform of the wavelet function. The Daubechies order 4 wavelet with orthogonal basis is chosen because of its similarity to SEM waveform [3]. Because the recorded HEO signal has been filter below 40Hz, so Table. I presents some frequency bands corresponding to different levels of decomposition for Daubechies order 4 wavelet with a re-sample frequency of 500 Hz. Since the family $\psi_{i,k}$ is an

TABLE I. FREQUENCY CORRESPONDING TO DIFFERENT LEVELS OF DECOMPOSITION.

Decomposed signal	Frequency range(Hz)
P_{10}	0-0.3488
D_{10}	0.3488-0.6975
D_9	0.6975-1.3951
D_8	1.3951-5.5804
D_7	5.5804-11.1607
D_6	11.1607-22.3214
D_5	22.3214-44.6429

orthogonal basis for $L(\mathcal{R})$, the concept of energy is linked with the usual notions derived from the Fourier theory. Then, the wavelet coefficients are given by $C_{D_i}(k) = \langle f_w(t), \psi_{i,k}(t) \rangle$. The energy at each resolution level $j=5,6, \dots, 10$ will be the energy of the detail signal D_i and the approximation signal P_{10} .

$$E_{D_j} = \sum_k |C_{D_j}(k)|^2, j = 5, 6, \dots, 10$$

$$E_{P_{10}} = \sum_k |C_{P_{10}}(k)|^2$$
(9)

Therefore, wavelet energy feature vector can be expressed as:

$$F_{WE} = [E_{P_{10}}, E_{D_{10}}, E_{D_9}, \dots, E_{D_5}]$$
(10)

B. Classifiers

1) *Support vector machine*: Support vector machine is a classic and popular machine learning method for classification. The problem of training SVM is usually to solve its dual problem, and the decision function is:

$$\text{sgn}(w^T \phi(x) + b) = \text{sgn}\left(\sum_{i=1}^l y_i a_i K(x_i, x) + b\right)$$
(11)

Here, LIBSVM package was used and radial basis function (RBF) was selected. The range of the penalty factor C and the parameter γ of RBF were set to $[0, 1024]$ and $[0.1, 2]$, respectively. All of the points of (C, γ) were tried to find the best training result.

2) *Graph regularized extreme learning machine*: Graph regularized extreme Learning Machine (GELM) is based the idea that similar samples should share similar properties and through adding a graph regularization term on the objective of conventional ELM to ensure the output of samples from the same class should be similar [13]. The standard ELM with K hidden nodes with activation function $g(x)$ can be modeled as following:

$$\sum_{j=1}^K \beta_j g_j(x_i) = \sum_{j=1}^K \beta_j g(w_j \cdot x_i + b_j)$$

$$= t_i, i = 1, \dots, N$$
(12)

where $x_i = (x_{i1}, x_{i2}, \dots, x_{id})^T$ and $t_i = (t_{i1}, t_{i2}, \dots, t_{im})^T$ form the training data $L = \{(x_i, t_i) | x_i \in R^d, t_i \in R^m\}$. The above N equations can be written as a matrix formulation as follows:

$$H\beta = T$$
(13)

So the output weight of ELM can be determined by Eq. (14), in which H^\dagger is the Moore-Penrose generalized inverse of H .

$$\beta^* = \arg \min_{\beta} \|H\beta - T\|_2^2 = H^\dagger T$$
(14)

Suppose that y_i and y_j are the output vectors for h_i and h_j mapped by output weight matrix β , $h_i = (g_1(x_i), \dots, g_K(x_i))^T$ and $h_j = (g_1(x_j), \dots, g_K(x_j))^T$. The goal of GELM is to ensure that if two inputs x_i, x_j are from the same class, their outputs should be similar to each other. So we want to minimize the following objective function with the adjacent W :

$$\min \sum_{i,j} \|y_i - y_j\|_2^2 W_{ij} = \text{Tr}(YLY^T)$$
(15)

where $Y = H\beta$, and adjacent W is defined as follows:

$$W_{ij} = \begin{cases} 1/N_t, & \text{if both } h_i \text{ and } h_j \text{ belong to the } t\text{th class} \\ 0, & \text{otherwise;} \end{cases}$$
(16)

By incorporating Eq. (15) and another regularization term into conventional ELM model, the objective function of GELM is:

$$\min_{\beta} \|H\beta - T\|_2^2 + \lambda_1 \text{Tr}(H\beta L\beta^T H^T) + \lambda_2 \|\beta\|_2^2$$
(17)

By setting the differentiate of above objective function with respect to β as zero, we have

$$\beta = (HH^T + \lambda_1 HLLH^T + \lambda_2 I)^{-1} HT \quad (18)$$

Eq. (18) makes the output weight matrix calculated directly.

III. MATERIAL

A. Experiment

1) *Subjects*: Six normal students (4 male and 2 female, aged 22 ± 3) were recruited from Shanghai Jiao Tong University. Because the appearing of SEM was known to commonly occur in the beginning of sleep, and to ensure that the time epochs of SEM in every experiment were many enough, the students who had good regular sleeping habits were selected and the starting time of every experiment was one hour before their afternoon nap time about from 12:30 pm to 14:30 pm.



Fig. 7. Driving simulation environment

2) *Procedure*: The driving simulator used in the experiment (Fig. 7), had a four-lane national highway with road signs and scenarios. Prior to the beginning of the experiment, the subject was required to do a 'warm-up and training' session lasting 10 min to be familiar with the vehicle controls. In this simulated scene, subjects as drivers were required to keep alertness all time as soon as possible and trying to suppress his/her sleepiness to avoid any traffic accidents. Each driving simulator experiment lasted for more than two hours.

3) *Data recording*: EOG were recorded by the NeuroScan system at a sampling rate 1000Hz, and a bandpass filtering between 0 and 40 Hz was done to remove irrelevant noise signals. The electrodes placement was the same as the conventional ones in EOG experiments analysis [3]. A camera was set to monitor the subject's face to clearly recognize the opening or closing state of eyes. The subject's face image from the camera and the real-time displaying of EOG signal in SCAN software were displayed at the same computer screen at the same time. And through the computer screen recording software, both together were recorded into the same video file. So with this video file, we could determine the eye state when SEM occurred. Because the waveform of VOR (Vestibulo-ocular reflex) is very similar to the SEM, so to avoid the error identification of SEM, subjects were instructed to keep their head motionless on the seat during the driving simulator experiment.

B. SEMs characteristics

SEMs are considered as reliable signs that sleep onset period has been entered, usually appear during the transition from wakefulness to sleep [2, 16]. According to our experiments, the following characteristics were verified:

1) *SEMs most occur with eyes closed*: Through looking back at the recorded video files, in which both the eye state (open or closed) and the EOG signal could be observed at the same moment, the conclusion of this check was that SEMs almost completely occurred when eyes closed and few occurred during the period of continuous frequent overlong blinks. Marzano *et.al.* mentioned that 'slow ocular activity (SEM) could be a valid indicator of alertness only when eyes are closed and people are already falling asleep' [16]. Even though SEM happened with eyes closed, but it is still useful in driving fatigue detection.

Fig. 8 gives an example of long eyes closures with SEM appearing when the driver is very sleepy, while when the driver is awake but closes eyes due to other reasons the SEM will not appear. For overlong eyelid closures, there are no good methods to detect it. The conventional detection method is only according to the waveform in VEO, but it can not distinguish from an upward glance followed by a downward glance (Fig. 8) [8, 9]. And in the condition of serious squint, the waveform caused by eyes closing and then the following waveform caused by eyes opening in VEO were not obvious. However, at this movement, the waveform of SEM in the HEO was very clear and easy to recognize. So detecting SEMs in HEO was very significant to detect driver's fatigue and can distinguish from the driver's state with eyes closed but not sleepy.

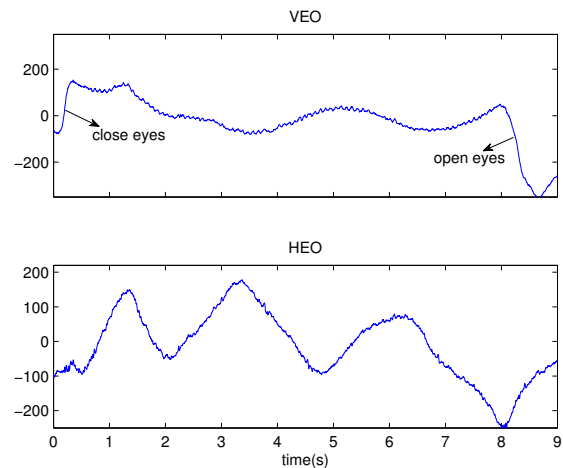


Fig. 8. SEMs during a overlong eyelid closure when sleepy

When the driver is awake with eyes opening, fast eye movement and fixation are the main eye movements and there also exist more complicated eye movements which are caused by eye tracking the activities of objects.

2) *Relatively loose experiment restrictions*: Though the subjects were required to restrain drowsiness as far as possible, due to the simulated driving condition was much looser than real driving condition, the long time dozes with eyes closed

(most in the range of 4-10s, and few in 10-13s, and very few in 13-20s) were permissible and conducive to investigate the characteristics of EOG signals, because these long time epochs with eye closed (when SEM occurred) usually were not allowed to happen and would be big dangerous occurrences in real-world driving.

IV. RESULTS

For bio-signal, individual variation usually exists, and the skin impedance value and the different skull structure will cause some signals' amplitude differences in different subjects. Therefore, training and testing were done within the individual in this study.

In section III, we mentioned that the restriction of simulated driving experiments is relatively loose and allow the subjects have dozens with some long times. But the whole time length of SEMs was still very shorter than the whole time length of non-SEMs, and the ratio between the two could be as high as 300:1 (non-SEMs:SEMs) (Table II). This is a problem of samples imbalance. To deal with imbalance problem, we use the two main schemes [7]: 1) Under-sampling the large class until it matches the size of the small class. 2) Over-sampling the small class until it contains as many samples as the other class.

TABLE II. THE RATIO BETWEEN THE SEMs AND NON-SEM s FOR SIX SUBJECTS' SESSIONS

Session	SEMs(sec)	non-SEMs(sec)	Ratio
1	451.4	6771	15:1
2	23.6	7209	305:1
3	182.7	7124	39:1
4	30.9	7201	233:1
5	449.4	7190	16:1
6	213.2	7038	33:1

For the under-sampling method, all SEM epochs and non-SEM epochs were divided into many 2s window data samples with a sliding step ($s=0.3s$). And after that if the number of SEMs with 2s time length was N , and the number of non-SEMs was M , so the first $N/2$ SEMs were put into training set. Because M was far larger than N , so the random selected $N/2$ non-SEMs were also put into training set. Then the rest $N/2$ SEMs and the random selected $N/2$ non-SEMs from the rest after the previous selection were put into testing set. Through this training and testing of 10 times, the mean performance of features was obtained by three classifiers respectively. To evaluate the performance of the features and classifiers, the following indicators were used to measure it.

$$\text{Agreement}=(TP + TN)/\text{total number of samples}*100\%$$

$$\text{Sensitivity}=TP/(TP + FN)*100\%;$$

$$\text{Selectivity}=TP/(TP + FP)*100\%;$$

where, TN is the number of negative samples correctly classified, FP is the number of negative samples incorrectly classified as positive, FN is the number of positive samples

incorrectly classified as negative and TP is the number of positive samples correctly classified. In the following tables, WE represents wavelet energy features (F_{WE}), DF new defined features (F_{DF}) and BOTH means the combination of them. From Table III, we can find the overall performance of our

TABLE III. THE AGREEMENT OF THREE CLASSIFIERS OVER SIX SUBJECTS FOR THE UNDER-SAMPLING METHOD

Feature	Classifier	1	2	3	4	5	6
WE	SVM	80.2	80.1	87.8	81.1	85.9	86.5
	GELM	79.8	78.9	87.6	79.2	85.5	84.7
	KNN	74.9	69.1	83.6	70.0	78.7	82.9
DF	SVM	88.2	79.5	90.7	80.4	91.9	90.6
	GELM	87.8	81.4	89.5	81.3	91.5	89.9
	KNN	78.5	66.7	78.5	68.6	82.2	77.5
BOTH	SVM	90.6	89.9	92.2	90.8	92.6	91.2
	GELM	91.9	90.0	91.8	90.9	92.6	90.8
	KNN	79.0	81.2	80.3	81.4	85.2	80.2

new defined features is better than the only wavelet energy features, and by combination of this two features, the agreement value can be improved significantly. The next two tables (Table IV and Table V) give the corresponding sensitivity and the selectivity results of all subjects respectively. In general, the sensitivity results are a little sensitive to the kind of features and classifiers compared to the selectivity results.

TABLE IV. THE SENSITIVITY RESULTS FOR THE UNDER-SAMPLING METHOD

Feature	Classifier	1	2	3	4	5	6
WE	SVM	76.2	82.3	91.4	83.3	86.5	90.9
	GELM	74.4	82.9	90.1	83.9	88.2	90.8
	KNN	61.5	52.1	77.3	57.1	72.2	78.6
DF	SVM	89.5	78.5	93.9	75.5	92.7	92.8
	GELM	89.8	78.8	95.3	76.1	92.7	93.6
	KNN	67.2	50.1	69.5	58.5	73.1	72.4
BOTH	SVM	91.3	80.2	96.8	82.8	92.3	97.0
	GELM	91.8	82.6	96.7	84.5	92.5	97.1
	KNN	71.9	60.2	71.6	62.2	78.23	70.9

TABLE V. THE SELECTIVITY RESULTS FOR THE UNDER-SAMPLING METHOD

Feature	Classifier	1	2	3	4	5	6
WE	SVM	82.9	79.8	85.4	79.2	85.7	86.3
	GELM	83.5	76.8	81.8	78.2	84.2	82.8
	KNN	83.9	78.7	88.6	76.1	83.3	88.6
DF	SVM	82.9	88.2	88.3	88.1	91.4	89.2
	GELM	83.4	85.1	85.2	86.4	91.8	91.1
	KNN	83.2	77.5	85.0	78.5	89.6	86.9
BOTH	SVM	88.8	90.0	88.7	90.0	93.0	88.7
	GELM	88.6	86.3	86.2	87.3	92.8	86.2
	KNN	89.7	83.6	87.0	83.6	91.2	85.0

For the over-sampling method, the sliding step s was used to over-sampling the class of SEMs until it contained as many samples as the non-SEMs. The operation for this was that if the ratio between the non-SEMs and SEMs was $m:1$, then the time length of the sliding step was set to $2s/m$, which was the window time length divided by m . But the sliding step was only for the SEMs epochs not for non-SEMs epoches. Therefore, the number of SEMs was almost equal to the number of non-SEMs, and half of them respectively were put into training set and the rest of them into testing set. In the

TABLE VI. THE AGREEMENT RESULTS FOR OVER-SAMPLING METHOD

Feature	Classifier	1	2	3	4	5	6
WE	SVM	99.98	100	100	100	97.16	100
	GELM	99.99	100	100	100	99.67	100
	KNN	99.98	100	100	100	96.91	100
DF	SVM	99.96	100	100	100	99.91	100
	GELM	100	100	100	100	99.95	100
	KNN	99.95	100	100	100	99.91	100
BOTH	SVM	99.98	100	100	100	99.96	100
	GELM	99.99	100	100	100	99.97	100
	KNN	99.98	100	100	100	99.91	100

Table VI we can see, by over-sampling the SEMs epoches, the agreements of all subjects could become very high, compared to the under-sampling method. The reason for this results may be, on the one hand, to reach this size of non-SEMs the number of training samples was dramatically expanded, and on the other hand, by the very tiny time length of sliding step (such as $2s/305.5 = 0.0065s$), more similar SEMs were generated and thus easy to recognize. Another reason might be partly that the database was simple and small.

However, for the VOR, which is SEM-like eye movement, the algorithm still can not distinguish and the experiments limited the generation of VOR in order to determine the eye closed state when SEM occurred.

V. CONCLUSIONS

The occurrence of slow eye movement means that the driver is about to enter the initial stage of sleep, so it is extremely dangerous and in urgent need of detecting it. This study discusses the characteristics of slow eye movement in the driving simulation experiments and proposed new features based on wavelet singularity analysis and statistics to improve the detection effect of SEMs. Experiments results indicate new defined features are a little better than the wavelet energy, and the combination of wavelet energy features and new defended features can obtain better classification results than each single kind of features. In the real-world driving environment, there are more complicated eye movements such as VOR and smooth pursuit, which will bring difficulties for detecting SEMs. Therefore, that will be further studied for SEM recognition in our future work.

ACKNOWLEDGMENT

This work was partially supported by the National Natural Science Foundation of China (Grant No. 61272248), the National Basic Research Program of China (Grant No. 2013CB329401), and the Science and Technology Commission of Shanghai Municipality (Grant No. 13511500200), and the Open Funding Project of National Key Laboratory of Human Factors Engineering (Grant No. HF2012-K-01).

REFERENCES

[1] Marzano C, Fratello F, Moroni F, Pellicciari M C, Curcio G, Ferrara M, Ferlazzo F, De Gennaro L, *Slow eye movements and subjective estimates of sleepiness predict EEG power changes during sleep deprivation*, Sleep, 2007, 30(5): 610.

[2] De Gennaro L, Ferrara M, Ferlazzo F, Bertini M, *Slow eye movements and EEG power spectra during wake-sleep transition*, Clinical neurophysiology, 2000, 111(12): 2107-2115.

[3] Magosso E, Provini F, Montagna P, Ursino M, *A wavelet based method for automatic detection of slow eye movements: A pilot study*, Medical engineering physics, 2006, 28(9): 860-875.

[4] Daubechies I, *The wavelet transform, time-frequency localization and signal analysis*, IEEE Transactions on Information Theory, 1990, 36(5): 961-1005.

[5] Shin D, Sakai H, Uchiyama Y, *Slow eye movement detection can prevent sleep related accidents effectively in a simulated driving task*, Journal of sleep research, 2011, 20(3): 416-424.

[6] Hiroshige Y, *Linear automatic detection of eye movements during the transition between wake and sleep*, Psychiatry and Clinical Neurosciences, 1999, 53(2): 179-181.

[7] Japkowicz N, Stephen S, *The class imbalance problem: A systematic study*, Intelligent Data Analysis, 2002, 6(5): 429-449.

[8] Schleicher R, Galley N, Briest S, Galley L, *Blinks and saccades as indicators of fatigue in sleepiness warnings: looking tired?*, Ergonomics, 2008, 51(7): 982-1010.

[9] Jammes B, Sharabty H, Esteve D, *Automatic EOG analysis: A first step toward automatic drowsiness scoring during wake-sleep transitions*, Somnologie-Schlafforschung und Schlafmedizin, 2008, 12(3): 227-232.

[10] Bergasa L M, Nuevo J, Sotelo M A, Barea R, *Real-time system for monitoring driver vigilance*, IEEE Transactions on Intelligent Transportation Systems, 2006, 7(1): 63-77.

[11] Harrison Y, Horne J A, *Occurrence of 'microsleeps' during daytime sleep onset in normal subjects*, Electroencephalography and Clinical Neurophysiology, 1996, 98(5): 411-416.

[12] Boyle L N, Tippin J, Paul A, Rizzo M, *Driver performance in the moments surrounding a microsleep*, Transportation research part F: traffic psychology and behaviour, 2008, 11(2): 126-136.

[13] Peng Y, Wang S, Long X and Lu B L, *Discriminative Graph Regularized Extreme Learning Machine for Face Recognition*, To appear in Neurocomputing, 2013.

[14] Mallat S, Hwang W L, *Singularity detection and processing with wavelets*, IEEE Transactions on Information Theory, 1992, 38(2): 617-643.

[15] Sun Q, Tang Y, *Singularity analysis using continuous wavelet transform for bearing fault diagnosis*, Mechanical Systems and Signal Processing, 2002, 16(6): 1025-1041.

[16] Marzano C, Fratello F, Moroni F, Pellicciari M C, Curcio G, Ferrara M, Ferlazzo F, De Gennaro L, *Slow eye movements and subjective estimates of sleepiness predict EEG power changes during sleep deprivation*, Sleep, 2007, 30(5): 610.

[17] Li G, Chung W Y, *Detection of driver drowsiness using wavelet analysis of heart rate variability and a support vector machine classifier*, Sensors, 2013, 13(12): 16494-16511.